physics

MDPI

Article

Optical Medium Approach: Simplifying General Relativity and Nonlinear Electrodynamics for Educational Purposes

Saken Toktarbay [1,2], Nurzada Beissen [1], Manas Khassanov [1,*], Temirbolat Aitassov [3] and Amina Sadu [1]

1 Institute for Experimental and Theoretical Physics, Al-Farabi Kazakh National University, Almaty 050040, Kazakhstan; saken.toktarbay@kaznu.edu.kz (S.T.); nurzada.beissen@kaznu.edu.kz (N.B.); sadu_amina@live.kaznu.kz (A.S.)
2 Department of Physics, Kazakh National Women's Teacher Training University, Almaty 050000, Kazakhstan
3 Department of Mathematics, Physics and Informatics Teaching Methods, Abai Kazakh National Pedagogical University, Almaty 050010, Kazakhstan; temirbolat.aytasov@physics.kz
* Correspondence: khassanov.manas@kaznu.kz

Abstract: This paper explores the optical approach to simplifying complex concepts in general relativity (GR) and nonlinear vacuum electrodynamics. The focus is on using optical analogies to simplify the understanding of spacetime curvature and interactions in strong gravitational and magnetic fields. We demonstrate how applying concepts of effective refractive index can facilitate the teaching and comprehension of GR optical effects, such as gravitational lensing and the behavior of light around massive objects. Additionally, the paper covers the application of optical analogies in the context of nonlinear vacuum electrodynamics, showing how strong magnetic fields affect light propagation. This interdisciplinary approach provides a more natural understanding and modeling of complex physical phenomena, making them better accessible for study and teaching.

Keywords: optical medium approach; refractive indices; general relativity; nonlinear electrodynamics; educational methods in theoretical physics

check for updates

Citation: Toktarbay, S.; Beissen, N.; Khassanov, M.; Aitassov, T.; Sadu, A. Optical Medium Approach: Simplifying General Relativity and Nonlinear Electrodynamics for Educational Purposes. *Physics* **2024**, *6*, 1294–1305. https://doi.org/10.3390/physics6040080

Received: 18 September 2024
Revised: 4 November 2024
Accepted: 14 November 2024
Published: 5 December 2024

1. Introduction

Studying the effects of general relativity (GR), particularly its optical effects, presents a challenging task, primarily due to the need to explain spacetime curvature and utilize advanced mathematical tools [1]. It is possible to accurately describe the physical phenomena of spacetime using the field equations of GR. However, these equations possess a complex mathematical structure, and even the simplest geodesic equations generally lack analytical solutions. These complexities often become significant barriers in the educational process, especially when lacking enough knowledge in higher mathematics.

However, despite these challenges, there is a growing interest in including GR in school and university curricula, given its importance in modern physics and its practical applications in areas such as GPS (Global Positioning System) technology and astronomy [2]. Recent studies indicate that even high school students can develop a qualitative understanding of key GR concepts, provided the students have access to appropriate educational resources and support from the teachers [3,4].

There are various methods for teaching GR, including the use of numerical modeling and computer simulations [1,5]. However, many of these approaches remain challenging to grasp at a natural level, which limits their effectiveness for educational purposes. Research suggests that using more visual methods, such as optical analogies, can significantly enhance students' understanding of complex GR concepts by making them more accessible [6].

The purpose of using optical analogies, such as the refractive index, in the context of GR was first proposed by Igor Tamm [7], then by Nándor Balazs [8], and has been further developed in subsequent research [9–15]. Building on this studies, we demonstrate how the concept of an effective refractive index can be applied to model GR effects, such as the behavior of light near stationary and rotating massive objects, as well as in the case of nonlinear vacuum electrodynamics [16,17]. This underscores the value of this approach for modeling and teaching complex physical phenomena.

We show that using these analogies not only makes it more straightforward to understand complex GR concepts but also makes those concepts more accessible for teaching, potentially simplifying the learning process and increasing student interest in the topics. To this end, in this paper, we demonstrate how the examples and methods compiled can facilitate the educational process and make complex theoretical concepts more accessible to students and young researchers.

The current paper is organized as follows. Section 2 reviews the concept of the optical medium approach in the GR theory. In Section 3, we consider the effective refractive index in the case of spherical symmetric gravitational field. In Section 4, we study the refractive index and deflection angle for the rotating compact objects. In Section 5, we calculate the effective refractive index in nonlinear vacuum electrodynamics. The application of the considered method to magnetars is shown in Section 6. Finally, Section 7 contains a summary of the results.

2. The Concept of the Optical Medium Approach

The concept of the optical medium approach involves discarding some of the internal paradigms of a given theory and replacing them with a medium that has a corresponding refractive index n [18]. The refractive index can reproduce the optical effects derived from the theory. This concept allows for natural and visual representation of complex physical phenomena, making them more accessible for understanding and analysis.

In the case of GR, the internal paradigm is the curvature of spacetime. The curvature caused by massive objects affects the trajectories of light and matter, creating effects such as the behavior of light near massive objects; see Figure 1, right. In the optical medium approach, one can represent this curved geometry as a medium with a variable refractive index, which often depends on mass and distance [19]; see Figure 1, left. This allows using of optical analogies to understand and model the effects of GR without delving into the complex mathematical aspects of the theory. Many studies have been conducted using the optical medium approach, which enables the study of motion with high accuracy without the need to solve geodesic equations [9,11]. This method applies not only to homogeneous media in spherically symmetric spacetime but also to the various scenarios of gravitational fields of compact objects with quadrupole moments [14,15,20,21].

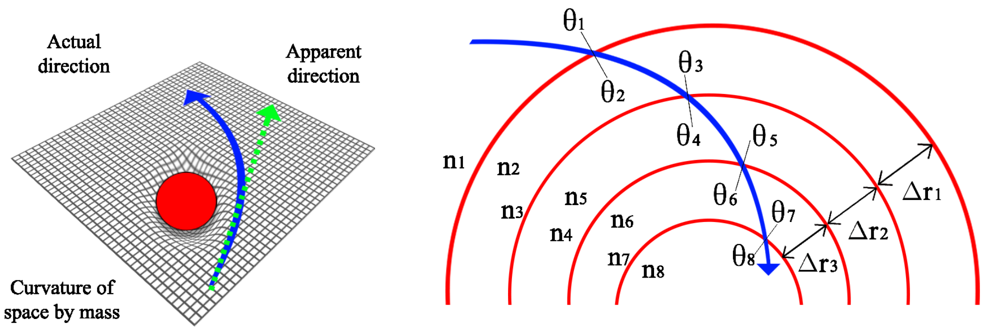

Figure 1. Demonstration of the refraction of light by a gravitational field. **Left**: representation by spacetime curvature. The red ball shows the massive body, the blue and green arrows show the light direction as indicated. **Right**: representation by an optical medium. The blue arrow shows the light direction. The numbers indicate the layers (in red).

Similarly, in the case of the nonlinear theory of vacuum electrodynamics, the internal paradigm involves the formation of electron–positron pairs in the presence of a strong magnetic field [22]. In this context, the optical medium approach allows us to represent the vacuum as a nonlinear medium with a refractive index that depends on the intensity of the magnetic field [17]. This helps us straightforwardly understand how strong fields affect the properties of the vacuum and particle interactions.

One of the key advantages of the optical medium approach is the ability to simulate gravitational fields in laboratory conditions using optically non-uniform media. This allows for the visual reproduction of effects similar to those described by the theory of gravitational lensing.

In Ref. [23], methods for forming a spherical layered structure through the adjustment of the temperature regime of a metal sphere placed in a gas environment are proposed. Since the refractive index of the gas changes with temperature, heating or cooling the sphere allows for the creation of the needed temperature distribution and the achievement of the necessary refractive index profile $n(r)$, with r denoting the distance. However, the main challenge of this model lies in accurately reproducing the required temperature distribution in the gas.

Instead of gas, it is more convenient to use a transparent solid material with a pronounced temperature dependence of the refractive index; see Figure 2. For example, in Ref. [24], plexiglass was used. Using such a material is more straightforward than gas environments; however, even in this case, only a qualitative reproduction of the optical characteristics of gravitational lenses can be achieved, as it is complicated to ensure an accurate temperature distribution throughout the volume of the lens. These complications can be overcomed by avoiding the creation of a non-uniform medium and instead reproducing only the required deflection angle, $\theta(r)$, using a lens made of homogeneous transparent material with a specially designed surface geometry, the shape of which was calculated in Refs. [23,24].

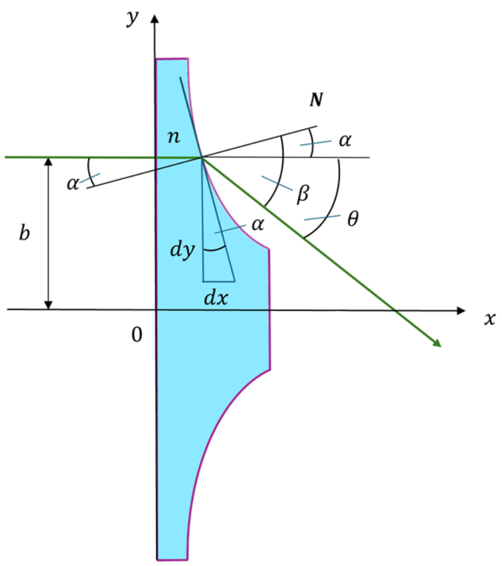

Figure 2. Cross-section of a gravitational lens model of plexiglass on the xy-plane. The green arrow indicates the light coming from the left at a distance b from the x-axis. N denotes the surface normal, n is the refractive index, θ is the deflection angle, dx and dy are the projections of the light path along the x and y axes, respectively, associated with the angle α.

The shape of a lens that provides a specified refraction law $\theta(y)$, where y is the parameter that associated to the impact parameter b. For simplicity, one of the lens surfaces is made flat, allowing rays traveling parallel to the x-axis to pass through the entry surface without deviation. The shape of the refracting (exit) surface $x = x_S(y)$ is determined based on Snell's law: $n \sin\alpha = \sin\beta$, where the angles α and β are measured relative to the surface normal N. Given that $\beta = \alpha + \theta(y)$ and $\tan\alpha = dx_S/dy$, the wanted equation for the surface can be obtained as

$$x_S(y) = x_0 - \int_0^y \frac{\sin\theta(y')}{n - \cos\theta(y')}\,dy'. \tag{1}$$

Expression (1) remains valid not only in the case of axial symmetry, but also in the case when the deflection angle θ depends not just on the impact parameter y, but on the azimuthal angle ϕ as well. However, in that case, the refractive surface of the lens $x = x_S(y,\phi)$ is no longer a surface of revolution.

In what follows, we analytically consider the methods for calculating the effective refractive index and deflection angle for some cases, as these quantities play a key role in conducting demonstrative experiments.

3. The Effective Refractive Index in the Case of the Schwarzschild Solution

The solution to the Einstein field equation for a static and spherically symmetric gravitational field, known as the Schwarzschild solution [25], has the following form:

$$ds^2 = (1 - r_g/r)c^2dt^2 - r^2\left(\sin^2\theta d\phi^2 + d\theta^2\right) - \frac{dr^2}{1 - r_g/r}, \tag{2}$$

where $r_g = 2GM/c^2$ is the so-called Schwarzschild radius with G the Newtonian gravitational constant, M the object mass, and c the speed of light, and t denotes the time. Throughout the paper, the da^2 denotes the differential squared, $(da)^2$, not the differential of the squared variable. The line element (2) can be expressed in isotropic form $ds^2 = f(\rho)dt^2 - d\boldsymbol{\rho}^2$ by introducing a new radius coordinate ρ using the transformation

$$r = \rho\left(1 + \frac{r_g}{4\rho}\right)^2 \tag{3}$$

since in the isotropic form, the metric has the same coefficient for all spatial coordinates (ρ, θ, φ) [14,25].

Upon the transformation (3), the metric reads

$$ds^2 = \left(\frac{1 - r_g/(4\rho)}{1 + r_g/(4\rho)}\right)^2 c^2dt^2 - \left(1 + \frac{r_g}{4\rho}\right)^4\left(d\rho^2 + \rho^2(\sin^2\theta d\phi^2 + d\theta^2)\right), \tag{4}$$

where $d\rho^2 + \rho^2(\sin^2\theta d\phi^2 + d\theta^2)$ has the dimension of the square of the infinitesimal length vector, $d\boldsymbol{\rho}^2$. The speed of light in isotropic coordinates can be determined as follows:

$$v(\rho) = \left|\frac{d\vec{\rho}}{dt}\right| = \frac{(1 - r_g/(4\rho))c}{(1 + r_g/(4\rho))^3}. \tag{5}$$

Using inverse coordinate transformation, $\rho = \frac{1}{2}\left((r - r_g/2) + \sqrt{r(r - r_g)}\right)$, building on the work of [14] one can express the velocity of light as a function of r:

$$v(r) = v(\rho)\frac{dr}{d\rho} = \frac{c(r - r_g)}{r}. \tag{6}$$

Defining $n(r) = c/v(r)$, the resulting equation provides the effective refractive index for light in a Schwarzschild gravitational field:

$$n(r) = \frac{r}{r - r_g}. \tag{7}$$

The effective refractive index $n(r)$ (7) from the Schwarzschild solution reveals how gravitational fields influence light propagation. As r approaches the Schwarzschild radius r_g, $n(r)$ increases dramatically, indicating stronger gravitational effects. Under the far-field approximation, the expression (7) can be expressed as

$$n(r) = 1 + r_g/r. \tag{8}$$

Using the effective refractive index, one can derive characteristics of GR effects, such as the deflection angle, straightforwardly compared to solving geodesic equations, as demonstrated in Appendix A.

Having established the effective refractive index in the Schwarzschild metric, one can extend this approach to other solutions of the Einstein field equations.

4. The Effective Refractive Index in the Case of a Rotating Object

For practical purposes, the linearized Kerr metric [26] satisfactorily describes the gravitational field around a rotating star or planet. To simplify the problem, one can consider the deflection in the equatorial plane using this linearized Kerr metric:

$$ds^2 \approx -\left[\left(1 - \frac{r_g}{r}\right) + \frac{2r_g a}{r}\frac{d\varphi}{cdt}\right]c^2dt^2 + \frac{1}{(1 - r_g/r)}dr^2 + r^2(d\theta^2 + d\varphi^2), \tag{9}$$

where $a = J/m$ represents the spin parameter of the rotating object, which is a measure of the angular momentum per unit mass m. The multiplier $d\varphi/(c \cdot dt)$ denotes a frame-dragging parameter due to the rotating body.

By using the same transformation (3) to convert to the isotropic form and performing the same operations as in the case of the Schwarzschild solution, one derives expressions for the effective refractive index in the case of a rotating object [10]:

$$n(r,\theta) = \frac{r}{r - r_g} \cdot \left[1 + \frac{a}{c}\frac{r_g}{r - r_g}\frac{d\varphi}{dt}\right]^{-1/2}. \tag{10}$$

The frame-dragging parameter for a slowly rotating mass in the equatorial plane (at $\theta = \pi/2$) can be obtained by applying the principle of conservation of momentum and energy for photons. These conserved quantities can be expressed in terms of the covariant components of the metric $g_{\mu\nu}$ (with the Greek letter indices taking the time and space coordinates):

$$E = -g_{tt}\frac{dt}{d\lambda} - g_{t\varphi}\frac{d\varphi}{d\lambda}, \tag{11}$$

$$L = g_{\varphi\varphi}\frac{d\varphi}{d\lambda} + g_{t\varphi}\frac{dt}{d\lambda}. \tag{12}$$

where λ is the parameter by which the trajectory of light is parametrized. Expressing $d\varphi/d\lambda$ and $dt/d\lambda$ from Equations (11) and (12), one derives the relationship

$$\frac{d\varphi}{dt} = \frac{g_{t\varphi}E + g_{tt}L}{g_{\varphi\varphi}E + g_{t\varphi}L}. \tag{13}$$

By utilizing the relationship between E and L through the impact parameter $b = L/E$, and substituting the components of the Kerr metric, one obtains expressions for the frame-dragging parameter:

$$\frac{d\varphi}{dt} = \frac{r_g a + (r - r_g)b}{r^3 - r_g ab}c. \tag{14}$$

Then, up to the first order in a, the refractive index in the equatorial plane becomes

$$n(r) = 1 + \frac{r_g}{r} + \frac{r_g ab}{r^3}. \tag{15}$$

The result (15) shows that the refractive index depends on the spin parameter a. When $a = 0$, it implies that the central gravitational body is non-rotating. In such a scenario, the refractive index reduces to the Schwarzschild form (8). Comparing Equations (8) and (15), one deduces that

$$n(r) = n_{\mathrm{Sch}}(r) \cdot [1 + \delta n_{\mathrm{rot}}(r)], \tag{16}$$

where $n_{\mathrm{Sch}}(r) = 1 + r_g/r$ is the main term corresponding to the static gravitational field, and $\delta n_{\mathrm{rot}}(r) = ab/\left[r^2(1 + r/r_g)\right]$ is the correction taking into account the influence of angular momentum within the weak field. The angle of gravitational light deflection corresponding to this refractive index is provided in Appendix B.

5. The Effective Refractive Index in Nonlinear Vacuum Electrodynamics

In classical electrodynamics, the propagation of light through a vacuum is unaffected by external magnetic fields. This is due to the linear nature of Maxwell's equations [27], which do not predict any interaction between the electromagnetic waves (light) and a static magnetic field. However, when considering the nonlinear electrodynamics of vacuum [16,17,28–41], the interaction between propagating light and external magnetic fields becomes possible due to higher-order corrections, leading to novel phenomena such as vacuum birefringence. Nonlinear electrodynamics extends the classical theory by incorporating higher-order corrections that become significant in strong electromagnetic fields. One such framework is generalized Born–Infeld (BI) electrodynamics [17,35], which introduces nonlinear terms in the Lagrangian to account for these effects. This theory predicts that the vacuum behaves like a nonlinear optical medium with properties dependent on the external field strength.

To understand how light propagates in such a nonlinear medium, consider the Lagrangian density of let us generalized BI electrodynamics:

$$\mathcal{L} = \xi^2 \left(1 - \sqrt{1 + \frac{2S}{\xi^2} - \frac{P^2}{\xi^2 \eta^2}} \right), \tag{17}$$

where $S = \frac{1}{4} F_{\mu\nu} F^{\mu\nu}$ and $P = \frac{1}{4} F_{\mu\nu} \tilde{F}^{\mu\nu}$ with $F_{\mu\nu}$ the electromagnetic tensor. The parameters ξ and η are constants characterizing the nonlinear properties of the vacuum. Specifically, ξ is related to the maximum possible field strength in BI electrodynamics, while η influences the birefringence effect in the presence of an external magnetic field.

In further calculations, we consider the background magnetic field $\mathbf{B_0}$ caused by a magnetic dipole. We focus on a simplified case when the light ray travels through the equatorial plane of the magnetic dipole, as illustrated in Figure 3.

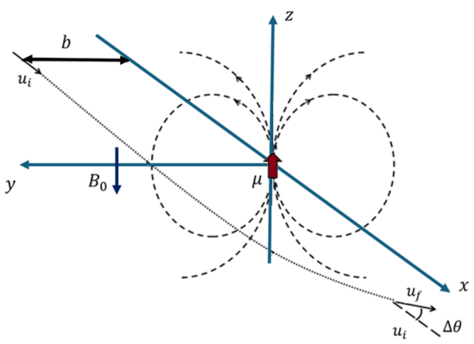

Figure 3. A schematic representation of a light ray traversing a magnetic dipole field. The red bold arrow indicates the dipole direction, while the dashed lines represent the magnetic field $\mathbf{B_0}$, u_i and u_f denote the initial and final position vectors along the photon's trajectory, μ represents the magnetic moment, and $\Delta\theta$ denotes the bending angle formed between the initial and final position vectors.

The refractive indices for two polarization modes (perpendicular and parallel to the background magnetic field) were derived in Ref. [17] from the eigenvalues of the polarization tensors:

$$n_\perp = \sqrt{1 + B_0^2/\xi^2}, \tag{18}$$

$$n_\parallel = \sqrt{1 + B_0^2/\eta^2}. \tag{19}$$

For relatively small values of the parameters B_0^2/ξ^2 and B_0^2/η^2, the effective refractive indices can be approximated as

$$n_\perp \approx 1 + \frac{B_0^2}{2\xi^2}, \tag{20}$$

$$n_\parallel \approx 1 + \frac{B_0^2}{2\eta^2}. \tag{21}$$

The components of effective refractive indices , $n_\perp$ and $n_\parallel$, derived from the nonlinear electrodynamics of vacuum illustrate how strong magnetic fields can alter light propagation. These indices show that the vacuum behaves as a nonlinear optical medium, leading to phenomena such as light deflection in Appendix C.

This approach not only transparentizes complex electromagnetic interactions in extreme conditions but also aligns with the broader purpose of using optical analogies to model and comprehend various physical phenomena.

6. Application on Magnetars

Magnetars are a type of neutron star known for their extremely strong magnetic fields, which can reach up to 10^{11}T on their surface [42,43]. Such fields are sufficient to exhibit the effects predicted by the nonlinear theory of vacuum electrodynamics. In addition to their intense gravitational fields, magnetars present a unique environment where both gravitational and electromagnetic influences must be considered to fully understand the behavior of light in the vicinity of magnetars [44]. The strong magnetic fields of magnetars are capable of inducing significant light bending, birefringence, and other nonlinear optical effects in the vacuum surrounding them. That is, the propagation of light near a magnetar is affected not only by the curvature of spacetime due to gravity but by the nonlinear interactions with the magnetic field as well [32].

By applying the optical medium approach, one can represent the effective refractive index around a magnetar as a combination of contributions from gravity and nonlinear electrodynamics [35]. Specifically, the total effective refractive index n_{eff} near the surface of a magnetar on the equatorial plane can be expressed as a product of the gravitational influence n_{gr}, and a correction factor δn_{mag} [33] as:

$$n_{\text{eff}}(r) = n_{\text{gr}}(r) \cdot [1 + \delta n_{\text{mag}}(r)], \tag{22}$$

where $n_{\text{gr}} = 1 + r_{\text{g}}/r$ corresponds to the Schwarzschild refractive index and $\delta n_{\text{mag}} = \left[1 + B_0^2/(2\xi^2)\right] r/(r + r_{\text{g}})$ is the correction factor due to the magnetic field. This form emphasizes the non-additive nature of the refractive index while providing a comprehensive view of light propagation near magnetars, considering both spacetime curvature and strong magnetic field effects.

7. Discussion

This paper has demonstrated the utility of the optical medium approach for understanding complex physical phenomena in Einstein's theory of gravity and nonlinear vacuum electrodynamics. Using optical analogies simplifies the representation and analysis of these phenomena, making them more accessible for understanding and teaching. Additionally, the use of materials such as plexiglass to model gravitational fields in laboratory conditions allows for a qualitative reproduction of gravitational lensing effects making this approach particularly useful for demonstrative experiments.

The optical medium approach is particularly useful for explaining the behavior of light around magnetars, which possess strong magnetic fields. Magnetars create unique conditions where both gravitational and electromagnetic effects are at play. Representing spacetime curvature and nonlinear vacuum effects through refractive indices provides a straightforward description of light behavior in such extreme environments. This approach enhances the understanding of magnetar physics and serves as an effective tool for educating students and young researchers.

Author Contributions: Conceptualization, M.K. and S.T.; methodology, M.K. and N.B.; validation, S.T.; formal analysis, M.K. and S.T.; investigation, T.A., A.S. and N.B.; writing—original draft preparation, M.K. and S.T.; writing—review and editing, S.T. and M.K.; resources, T.A. and A.S.; funding acquisition, N.B. and S.T. All authors have read and agreed to the published version of the manuscript.

Funding: This research was funded by the Ministry of Science and Higher Education of the Republic of Kazakhstan (Grant No. AP14972943).

Data Availability Statement: Not applicable.

Acknowledgments: We would like to extend our sincere appreciation to J.Y. Kim and M.E. Abishev for their valuable discussions.

Conflicts of Interest: The authors declare no conflicts of interest.

Appendix A

The trajectory of light in the equatorial plane can be described by the general expression for the refractive index [10,11,45]:

$$\Delta\theta = 2\int_b^\infty \frac{dr}{r\sqrt{\left(\frac{n(r)\cdot r}{n(b)\cdot b}\right)^2 - 1}} - \pi. \tag{A1}$$

Here, b is the impact parameter.

Let us rewrite the integral in Equation (A1) as follows (see Equation (7)):

$$I \equiv \int_b^\infty \frac{dr}{r\sqrt{\left(\frac{n(r)\cdot r}{n(b)\cdot b}\right)^2 - 1}} = n(b)\cdot b\int_b^\infty \frac{dr}{r^2\sqrt{\frac{1}{(1-r_g/r)^2} - \frac{b^2 r^{-2}}{(1-r_g/b)^2}}}. \tag{A2}$$

Introducing $q = r_g/r$ and $p = r_g/b$, the expression (A2) reads (here and in what follows, $n_b \equiv n(b)$),

$$I = \frac{n_b b}{r_g}\int_0^p \frac{(1-q)dq}{q\sqrt{1 - \left(\frac{q(1-q)}{p(1-p)}\right)^2}}. \tag{A3}$$

Returning to $p = r_g/b$, the quantity $1/(p(1-p))$ can be represented as

$$D \equiv \frac{b^2}{r_g(b - r_g)}. \tag{A4}$$

Then, one can represent the integral I (A2) as the sum of two integrals:

$$\begin{aligned} I &= \left(\frac{n_b b}{r_g}\right)\left[\int_p^0 \frac{(1-2q)dq}{\sqrt{1 - D^2q^2(1-q)^2}} + \int_0^1 \frac{qdq}{\sqrt{1 - D^2q^2(1-q)^2}}\right] \\ &= \left(\frac{n_b b}{r_g}\right) I_1 + \left(\frac{n_b b}{r_g}\right) I_2. \end{aligned} \tag{A5}$$

It is straightforward to identify

$$\frac{n_b b}{r_g} = \frac{1}{p(1-p)} = D. \tag{A6}$$

The first term in Equation (A6) can be calculated by changing q to $w = Dq(1-q)$, so that $dw = D(1-2q)dq$. Consequently, the upper and lower limits, $q = 0$ and $q = p$, change to $w = 0$ and $w = Dp(1 - r_g/b) = \frac{1}{p(1-p)} p(1-p) = 1$, respectively. That is,

$$\left(\frac{n_b b}{r_g}\right) I_1 = \int_0^p \frac{(1-2q)dq}{\sqrt{1 - D^2 q^2 (1-q)^2}} = \int_0^1 \frac{dw}{\sqrt{1-w^2}} = [\sin^{-1} w]_0^1 = \pi/2. \tag{A7}$$

Thus, based on Equation (A1), the deflection angle reads

$$\begin{aligned}
\Delta\theta &= 2\int_b^\infty \frac{dr}{r\sqrt{\left(\frac{n(r)\cdot r}{n(b)\cdot b}\right)^2 - 1}} - \pi \\
&= 2\left(\frac{n_b b}{r_g}\right) I_1 + 2\left(\frac{n_b b}{r_g}\right) I_2 - \pi \\
&= \pi + 2\left(\frac{n_b b}{r_g}\right) I_2 - \pi \\
&= 2\left(\frac{n_b b}{r_g}\right) \int_0^p \frac{q dq}{\sqrt{1 - D^2 q^2 (1-q)^2}}.
\end{aligned} \tag{A8}$$

Further assuming a weak-field approximation, the refractive index is given as $n(r) = 1 + p$. Under these conditions, one can approximate $1/D = p(1-p) \approx p$ and $q(1-q) \approx q$, assuming $q \ll 1$ and $p \ll 1$. Then,

$$\Delta\theta = 2D \int_0^p \frac{q dq}{\sqrt{1 - D^2 q^2 (1-q)^2}} \approx 2\int_0^p \frac{q dq}{\sqrt{p^2 - q^2}} = 2p = 2\frac{r_g}{b} = \frac{4GM}{c^2 b}. \tag{A9}$$

For a more detailed derivation of the gravitational light deflection angle, see [11].

Appendix B

The deflection angle can be computed using Equation (A1). When considering the rotational parameter a only to the first-order approximation, the linearized form of the deflection angle reads

$$\Delta\theta = \Delta\theta_0 + \Delta\theta_1, \tag{A10}$$

where the total deflection angle is represented by

$$\Delta\theta = \int_b^\infty \left[F(r) + aF_1(r)\right] dr, \tag{A11}$$

In this context, $\Delta\theta_0$ represents the deflection due to the Schwarzschild spacetime, given by Equation (A9). The function $F_1(r)$ is defined as

$$F_1(r) = -\frac{4m\left(b^2 + b\,r + r^2\right)}{b\,r^2 (b+r)\sqrt{r^2 - b^2}}. \tag{A12}$$

In the special case with $a = 0$, the deflection angle corresponds to that of Schwarzschild spacetime [11]. For the weak-field limit, assuming a slowly rotating object, we take $a^2/r^2 \ll 1$ and $1/a = 2m/R \ll 1$, where R represents the radius of the rotating body.

By evaluating the integral given in Equation (A11), the deflection angle can be determined up to the first order in the rotational parameter a. The second term of the integral contributes to the deflection due to the spacetime's rotation, leading to the frame-dragging effect captured by the term $\Delta\theta_1$, which is induced by the rotational components of the metric as seen in Equation (9). Consequently, the deflection angle becomes

$$\Delta\theta = \frac{4m}{R}\left(1 + \frac{a}{R}\right). \tag{A13}$$

The same results were obtained within alternative approaches in Refs. [9,13,14].

Appendix C

Here, to compute the deflection angle of light induced by a strong magnetic field, we will demonstrate another method based on the Gauss–Bonnet theorem (GBT) [46]. The GBT connects the geometry and topology of a surface, stating that the total Gaussian curvature of a compact, orientable 2- dimensional surface, combined with the geodesic curvature of its boundary, is proportional to the surface's Euler characteristic. As a consequence of this theorem, the angle of deflection of light is reduced to the calculation of the following integral [47]:

$$\Delta\theta_{\perp} = -\iint_{\mathcal{D}} \mathcal{K} d\mathcal{S}. \tag{A14}$$

The region $\mathcal{D}$ is characterized by its Gaussian curvature $\mathcal{K}$, which corresponds to a smoothly orientable curved surface $\mathcal{S}$ with an infinitesimal surface element $d\mathcal{S}$. The Gaussian optical curvature $\mathcal{K}$ is described in terms of the coordinates and refractive index:

$$\mathcal{K} = -\frac{n(r)\cdot n''(r)\cdot r - (n'(r))^2\cdot r + n(r)\cdot n'(r)}{n^4(r)\cdot r}, \tag{A15}$$

where the prime denotes differentiation with respect to the distance r.

Consider the background magnetic field caused by a magnetic dipole. In this case, the magnetic field of a magnetic dipole with the magnetic dipole moment $\mathbf{m}$, located at the origin, is given by [48]

$$\mathbf{B} = \frac{3(\mathbf{m}\cdot\mathbf{r})\mathbf{r}}{r^5} - \frac{\mathbf{m}}{r^3}. \tag{A16}$$

Unlike the isotropic electric field generated by a Coulomb charge, the magnetic field of a dipole is inherently anisotropic. Consequently, the bending angle of light depends on the orientation of the magnetic dipole relative to the incoming light ray. For simplicity, we consider the case where the light ray propagates through the equatorial plane of the dipole, and the magnetic dipole direction is aligned with the z axis, represented as $\mathbf{m} = \mu\hat{z}$, where μ represents the magnetic moment and $\hat{z}$ is a unit vector along the z-axis.

In the equatorial plane, Equation (A16) simplifies to

$$B_z = -\frac{\mu\hat{z}}{r^3}, \tag{A17}$$

where $r = \sqrt{x^2 + y^2}$. For the perpendicular mode (A14), using the effective refractive index, the Gaussian curvature is obtained as

$$\mathcal{K} = \frac{18\mu^2}{\xi^2 r^8}, \tag{A18}$$

where ξ is the parameter related to the maximum possible field strength in Born–Infeld (BI) electrodynamics.

Using the light-ray equation $r = b/\sin\varphi$, and applying both Equation (A18) and the expression for the area element $dS = n^2(r) r dr d\varphi$, one can now rewrite Equation (A14):

$$\Delta\theta_{\perp} = -\int_0^{\pi}\int_{\frac{b}{\sin\varphi}}^{\infty} \frac{18\mu^2}{\xi^2 r^8}\left(1 + \frac{\mu^2}{2\xi^2 r^6}\right)^2 r dr d\varphi \approx -\int_0^{\pi}\int_{\frac{b}{\sin\varphi}}^{\infty} \frac{18\mu^2}{\xi^2 r^7} dr d\varphi. \quad \text{(A19)}$$

As a result, the expression for the bending angle in the framework of generalized BI electrodynamics is given by

$$\Delta\theta_{\perp} = -\frac{15\pi}{16}\frac{\mu^2}{\xi^2 b^6}. \quad \text{(A20)}$$

The expression (A20) incorporates a negative sign, reflecting the fact that the deflection is oriented toward the magnetic dipole. This expression provides the bending angle of light within the framework of generalized BI nonlinear electrodynamics, accurate to the order of ξ^{-2}.

References

1. Stephani, H.; Kramer, D.; MacCallum, M.; Hoenselaers, C.; Herlt, E. *Exact Solutions of Einstein's Field Equations*; Cambridge University Press: New York, NY, USA, 2003. [CrossRef]
2. Kersting, M.; Henriksen, E.K.; Bøe, M.V.; Angell, C. General relativity in upper secondary school: Design and evaluation of an online learning environment using the model of educational reconstruction. *Phys. Rev. Phys. Educ. Res.* **2018**, *14*, 010130. [CrossRef]
3. Henriksen, E.K.; Bungum, B.; Angell, C.; Tellefsen, C.W.; Frågåt, T.; Vetleseter Bøe, M. Relativity, quantum physics and philosophy in the upper secondary curriculum: Challenges, opportunities and proposed approaches. *Phys. Educ.* **2014**, *49*, 678. [CrossRef]
4. Velentzas, A.; Halkia, K. The use of thought experiments in teaching physics to upper secondary-level students: Two examples from the theory of relativity. *Int. J. Sci. Educ.* **2013**, *35*, 3026–3049. [CrossRef]
5. Lehner, L. Numerical relativity: A review. *Class. Quant. Grav.* **2001**, *18*, R25–R86. [CrossRef]
6. Kaur, T.; Blair, D.; Moschilla, J.; Stannard, W.; Zadnik, M. Teaching Einsteinian physics at schools: Part 1. Models and analogies for relativity. *Phys. Educ.* **2017**, *52*, 065012. [CrossRef]
7. Tamm, I.E. The electrodynamics of anisotropic media in the special theory of relativity. *Zh. Rus. Fiz.-Khim. Obsch. Otd. Fiz. [J. Rus. Phys.-Chem. Soc. Phys. Sect.]* **1924**, *56*, 248–262. Available online (English translation): http://neo-classical-physics.info/uploads/3/0/6/5/3065888/tamm_-_ed_of_anisotropic_media_1924.pdf (accessed on 9 November 2024). (In Russian)
8. Balazs, N. Effect of a gravitational field, due to a rotating body, on the plane of polarization of an electromagnetic wave. *Phys. Rev.* **1958**, *110*, 236–239. [CrossRef]
9. Alsing, P. The optical-mechanical analogy for stationary metrics in general relativity. *Am. J. Phys.* **1998**, *66*, 779–790. [CrossRef]
10. Roy, S.; Sen, A.K. Trajectory of a light ray in Kerr field: A material medium approach. *Astrophys. Space Sci.* **2015**, *360*, 23. [CrossRef]
11. Sen, A.K. A more exact expression for the gravitational deflection of light, derived using material medium approach. *Astrophysics* **2010**, *53*, 560–569. [CrossRef]
12. Roy, S.; Sen, A.K. Study of gravitational deflection of light ray. *J. Phys. Conf. Ser.* **2019**, *1330*, 012002. [CrossRef]
13. Werner, M.C. Gravitational lensing in the Kerr–Randers optical geometry. *Gen. Rel. Grav.* **2012**, *44*, 3047–3057. [CrossRef]
14. Beissen, N.; Utepova, D.; Abishev, M.; Quevedo, H.; Khassanov, M.; Toktarbay, S. Gravitational refraction of compact objects with quadrupoles. *Symmetry* **2023**, *15*, 614. [CrossRef]
15. Beissen, N.; Utepova, D.; Kossov, V.; Toktarbay, S.; Khassanov, M.; Yernazarov, T.; Seydalieva, M. The influence of deformation in compact objects on redshift and radar echo delay. *Rec. Contrib. Phys.* **2024**, *88*, 4–11. [CrossRef]
16. Kruglov, S.I. Vacuum birefringence from the effective Lagrangian of the electromagnetic field. *Phys. Rev. D* **2007**, *75*, 117301. [CrossRef]
17. Kruglov, S.I. On generalized Born–Infeld electrodynamics. *J. Phys. A* **2010**, *43*, 375402. [CrossRef]
18. Plebanski, J. Electromagnetic waves in gravitational fields. *Phys. Rev.* **1960**, *118*, 1396–1408. [CrossRef]
19. Courbin, F.; Minniti, D. *Gravitational Lensing: An Astrophysical Tool*; Springer: Berlin/Hedelberg, Germany, 2002. [CrossRef]
20. Abishev, M.; Beissen, N.; Belissarova, F.; Boshkayev, K.; Mansurova, A.; Muratkhan, A.; Quevedo, H.; Toktarbay, S. Approximate perfect fluid solutions with quadrupole moment. *Int. J. Mod. Phys. D* **2021**, *30*, 2150096. [CrossRef]
21. Toktarbay, S.; Quevedo, H.; Abishev, M.; Muratkhan, A. Gravitational field of slightly deformed naked singularities. *Eur. Phys. J. C* **2022**, *82*, 382. [CrossRef]
22. Denisov, V.I.; Sokolov, V.A.; Vasili'ev, M.I. Nonlinear vacuum electrodynamics birefringence effect in a pulsar's strong magnetic field. *Phys. Rev. D* **2014**, *90*, 023011. [CrossRef]
23. Bliokh, P.V.; Minakov, A.A. *Gravitational Lenses*; Naukova Dumka: Kiev, Ukraine, 1989. (In Russian)

24. Simionato, S. Dark Matter and Gravitational Lensing as Teaching Tools for Physics and Astronomy. Ph.D. Thesis, Friedrich-Schiller-Universität Jena, Jena, Germany, 2022. Available online: https://www.db-thueringen.de/receive/dbt_mods_00052048 (accessed on 9 November 2024).
25. Landau, L.D.; Lifshitz, E.M. *The Classical Theory of Fields*; Pergamon Press PLC: Oxford, UK; Elsevier Ltd.: Oxford, UK, 2013. Available online: https://www.sciencedirect.com/book/9780080250724/the-classical-theory-of-fields (accessed on 9 November 2024).
26. Islam, J.N. *Rotating Fields in General Relativity*; Cambridge University Press: New York, NY, USA, 1985. [CrossRef]
27. Jackson, J.D. *Classical Electrodynamics*; John Wiley & Sons, Inc.: New York, NY, USA, 2021.
28. Heisenberg, W.; Euler, H. Folgerungen aus der Diracschen Theorie des Positrons. *Z. Phys.* **1936**, *98*, 714–732. [CrossRef]
29. Heisenberg, W.; Euler, H. Consequences of Dirac Theory of the Positron. *arXiv* **2006**, arXiv:physics/0605038. [CrossRef]
30. Denisov, V.I.; Dolgaya, E.E.; Sokolov, V.A. Nonperturbative QED vacuum birefringence. *J. High Energy Phys.* **2017**, *2017*, 105. [CrossRef]
31. Denisov, V.I.; Denisova, I.P.; Svertilov, S.I. Nonlinear electrodynamic effect of ray bending in the magnetic-dipole field. *Dokl. Phys.* **2001**, *46*, 705–707. [CrossRef]
32. Abishev, M.E.; Toktarbay, S.; Beissen, N.A.; Belissarova, F.B.; Khassanov, M.K.; Kudussov, A.S.; Abylayeva, A.Z. Effects of non-linear electrodynamics of vacuum in the magnetic quadrupole field of a pulsar. *Mon. Not. R. Astron. Soc.* **2018**, *481*, 36–43. [CrossRef]
33. Beissen, N.; Yernazarov, T.; Khassanov, M.; Toktarbay, S.; Taukenova, A.; Talkhat, A. Bending of light by magnetars within generalized Born–Infeld electrodynamics: Insights from the Gauss-Bonnet theorem. *Symmetry* **2024**, *16*, 132. [CrossRef]
34. Kim, J.Y.; Lee, T. Light bending by nonlinear electrodynamics under strong electric and magnetic field. *J. Cosmol. Astropart. Phys.* **2011**, *2011*, 017. [CrossRef]
35. Kim, J.Y. Deflection of light by magnetars in the generalized Born–Infeld electrodynamics. *Eur. Phys. J. C* **2022**, *82*, 485. [CrossRef]
36. Kruglov, S.I. On generalized ModMax model of nonlinear electrodynamics. *Phys. Lett. B* **2021**, *822*, 136633. [CrossRef]
37. Kruglov, S.I. Notes on Born–Infeld-type electrodynamics. *Mod. Phys. Lett. A* **2017**, *32*, 1750201. [CrossRef]
38. Kruglov, S.I. Born–Infeld-type electrodynamics and magnetic black holes. *Ann. Phys.* **2017**, *383*, 550–559. [CrossRef]
39. Kruglov, S.I. Magnetized black holes and nonlinear electrodynamics. *Int. J. Mod. Phys. A* **2017**, *32*, 1750147. [CrossRef]
40. Kruglov, S.I. Nonlinear electrodynamics and magnetic black holes. *Ann. Phys.* **2017**, *529*, 1700073. [CrossRef]
41. Beissen, N.; Abishev, M.; Toktarbay, S.; Yernazarov, T.; Aimuratov, Y.; Khassanov, M. Nonlinear electrodynamical lensing of electromagnetic waves on the dipole magnetic field of the magnetar. *Int. J. Mod. Phys. D* **2023**, *32*, 2350106. [CrossRef]
42. Manchester, R.N. Pulsars. In *Gravitational Radiation, Collapsed Objects and Exact Solutions. Proceedings of the Einstein Centenary Summer School, Perth, Australia, 01 January, 1979*; Edwards, C., Ed. Springer: Berlin/Heidelberg, Germany, 2005; pp. 34–66. [CrossRef]
43. Takibayev, N.; Nasirova, D.; Katō, K.; Kurmangaliyeva, V. Excited nuclei, resonances and reactions in neutron star crusts. *J. Phys. Conf. Ser.* **2018**, *940*, 012058. [CrossRef]
44. Riffert, H.; Meszaros, P. Gravitational light bending near neutron stars. I. Emission from columns and hot spots. *Astrophys. J.* **1988**, *325*, 207–217. [CrossRef]
45. Born, M.; Wolf, E. *Principles of Optics: Electromagnetic Theory of Propagation, Interference and Diffraction of Light*; Pergamon Press/Elsevier: Oxford, UK, 2013. Available online: https://www.sciencedirect.com/book/9780080264820/principles-of-optics (accessed on 9 November 2024).
46. Gibbons, G.W.; Werner, M.C. Applications of the Gauss Bonnet theorem to gravitational lensing. *Class. Quant. Grav.* **2008**, *25*, 235009. [CrossRef]
47. Ishihara, A.; Suzuki, Y.; Ono, T.; Asada, H. Finite-distance corrections to the gravitational bending angle of light in the strong deflection limit. *Phys. Rev. D* **2017**, *95*, 044017. [CrossRef]
48. Jusufi, K.; Övgün, A.; Saavedra, J.; Vásquez, Y.; Gonzalez, P. Deflection of light by rotating regular black holes using the Gauss-Bonnet theorem. *Phys. Rev. D* **2018**, *97*, 124024. [CrossRef]